A Study of Ship's Frictional Resistance in Extremely Shallow Water

Zeng, Qingsong; Hekkenberg, Robert; Thill, Cornel

Important note
To cite this publication, please use the final published version (if applicable).
Please check the document version above.

OMAE2019-95076

A STUDY OF SHIP'S FRICTIONAL RESISTANCE IN EXTREMELY SHALLOW WATER

Qingsong Zeng[1], Robert Hekkenberg, Cornel Thill
Delft University of Technology
2628CD, Delft, the Netherlands

ABSTRACT

In ship model tests, a model-ship correlation line (e.g., the ITTC57 formula) is used to calculate the frictional resistance of both the ship and its scaled model. However, this line is designed for deep water and the effects of water depth is not considered. Research has been conducted to improve the correlation line in shallow water, but studies of the extremely shallow water case (depth/draft, $h/T < 1.2$) are rare. This study focuses on the friction of two ship types in extremely shallow water, where the ship's boundary layer cannot develop freely. The physical details are analyzed based on the data generated with Computational Fluid Dynamics (CFD) calculations. The results show that for certain ship types at the same Reynolds number, the frictional resistance becomes smaller when the water is shallower. The geometry of the ship, in addition to the Reynolds number, becomes essential to the prediction of ship's friction in extremely shallow water. Therefore, this scenario is different from intermediate shallow and deep water, and the prediction method should be considered separately. The data and analysis shown in this study can help to improve the understanding and prediction of ship's frictional resistance in extremely shallow water.

Keywords: Frictional resistance; Extremely shallow water; Wigly hull; KVLCC2

INTRODUCTION

Inland shipping plays an important role in the transportation of passengers and cargo. Predicting ship's resistance accurately considering the effects of the waterway is essential to build an efficient ship.

Performing model tests is one of the important approaches for predicting a ship's resistance. In the commonly accepted approach, a model-ship correlation line (e.g., the ITTC57 formula [1]) is used to calculate the frictional resistance of both the ship and its scaled model. However in shallow water, limited space leads to a higher overspeed of the water around a hull. Moreover, due to a condition of zero tangential velocity on the water bottom, an extra boundary layer is formed. The higher overspeed and the extra boundary layer results in a thinner ship boundary layer compared to deep water. A higher velocity gradient in boundary layer is therefore achieved and leads to a higher shear stress on ship surface. Consequently, the correlation line derived from deep water starts to show large errors [2]. The prediction method of frictional resistance in shallow water needs to be improved.

Researchers have been working on this topic for about one century trying to find practically useful predictions for resistance in shallow water. However, studies in the extremely shallow water case where the ratio of water depth to ship draft (h/T) less than 1.2 are rare. In the researches of Schlichting [3] and Lackenby [4], h/T is always larger than 1.3. The method of Jiang [5] applies only for $h/T \geq 1.5$. The study of Raven [6] investigated lower h/T, but the number is still above 1.2.

It should be pointed out that extremely shallow water is commonly found in many inland waterways [7]. The conventional prediction of the frictional resistance derived from deep water and/or intermediate shallow water will not be accurate enough in extremely shallow water. The authors simplified the case into a 2D condition with the flow passes between two parallel walls [8] to study the boundary layer in shallow water.

---

[1] Contact author: Q.Zeng@tudelft.nl

Whereas, more phenomena can be observed at a 3D condition which will be introduced in this paper.

In this study, double-body computations are applied to reveal the physics of how a ship's friction changes in extremely shallow water scenarios. A Wigley hull and the KVLCC2 are used and the effects of a ship's geometry on friction are also analyzed. With the results and discussions, this study is expected to add new information and achieve a better understanding of the prediction of ship's frictional resistance in extremely shallow water.

METHOD

Two well-known and but contrasting ships, a Wigley hull and the KVLCC2, are analyzed through CFD calculations. Compared with the Wigley hull, the KVLCC2 has a much larger block coefficient and a large area of flat bottom. These features will influence the frictional resistance in extremely shallow water. In this part, details of the main dimensions of these two ships are presented, followed by the code verification and validation.

Models

The surface of the Wigley hull applied in this study is defined by the formula

$$y = \frac{B}{L}\left(1-\left(\frac{2x}{L}\right)^2\right)\left(1-\left(\frac{z}{T}\right)^2\right), \tag{1}$$

where B is the ship beam, L the ship length, and x, y, z are the coordinates at three directions. The origin is chosen at the intersection of the ship's midsection, ship's centerline, and the plane of still water surface. The x is positive forward, y is positive port and z is positive upward. As a 2.5m-length Wigley model was used in the experiments performed by Kajitani, et al. [9], for possible comparisons with the test data in this and future studies, the visual model with the same dimensions was built.

Similarly, a 1/58 model of the KVLCC2 is used in the tests of Kim, et al. [10], a numerical model with the same size was built and its main dimensions are listed in Table 1, together with the dimensions of the Wigley hull. The under-water part of the sections of each ship is depicted in Figure 1. To make a distinct comparison, the Wigley hull is shown at the same draft as the KVLCC2.

Table 1 Main dimensions of the Wigley hull and the 1/58 scaled KVLCC2

	Unit	Wigley hull	1/58 KVLCC2
L_{pp}	m	2.500	5.5172
B	m	0.250	1.0000
T	m	0.156	0.3586
C_B	-	0.445	0.8098

Setup of computations

Double-body computations are used to generate the frictional resistance of the ships. A commercial RANS code, Ansys Fluent (version 18.1), is applied. The numerical calculations are steady-state and the type of structured mesh is applied. The method of "Coupled" is used as the scheme of the pressure-velocity coupling and the discretization of gradient is "Least Squares Cell-Based". "Second Order Upwind" is applied for the discretization of momentum, turbulent kinetic energy, and specific dissipation rate. The SST k-ω model, which accounts for the transport of the turbulence shear stress in the definition of the turbulent viscosity and is considered to be reliable for adverse pressure gradient flows [11], is chosen as the turbulence model in this study.

The Reynolds numbers spread from lg(Re) = 5.8 to lg(Re) = 9.2, as shown in Table 2, which cover the range from ship models to full-scale ships. Four water depths are chosen in this study (Table 3), where the cases with h/T = 1.1 and h/T = 1.05 are both extremely shallow water scenarios. The deep water case and the case with h/T = 1.2 are used for comparison
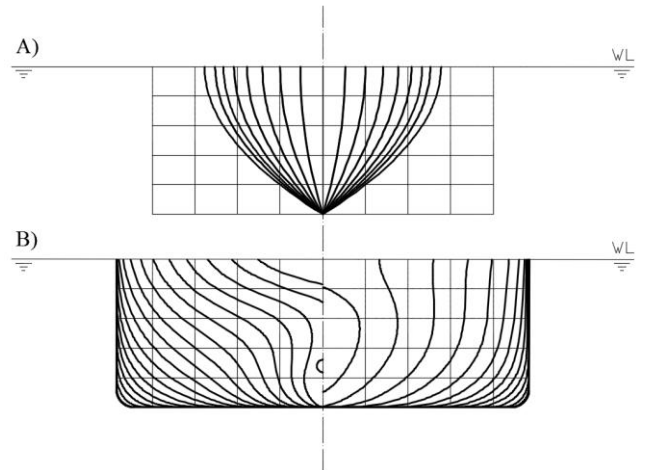

Figure 1. The sections of A) the Wigley hull, B) the KVLCC2

Table 2 The Reynolds number (Re) chosen in this study

No.	lg(Re)
1	5.8
2	6.0
3	6.2
4	6.4
5	6.6
6	6.8
7	7.2
8	7.6
9	8.0
10	8.4
11	8.8
12	9.2

Table 3 The selected water depths

No.	h/T
1	15.0 (deep)
2	1.2
3	1.1
4	1.05

(h: Water depth; T: Draft of the ship)

The computation domain extends L_{pp} in front of the ship and $3 L_{pp}$ at the back. The depth of the water (h) is determined by h/T. The position of the "Side" boundary should be decided carefully because if such boundary is too close to the ship, unexpected blockage effects will be caused. A short discussion about this problem will be shown later. The boundary conditions are shown in Figure 2 and the mesh around the ship hull is shown in Figure 3.
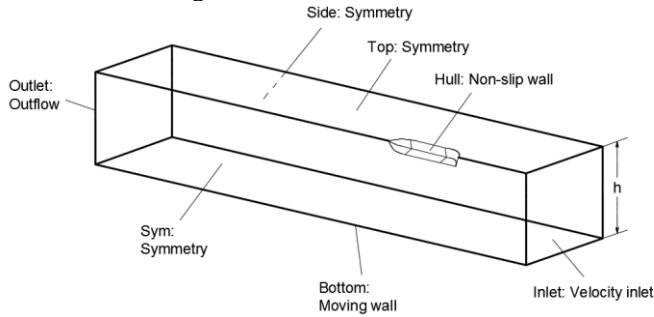

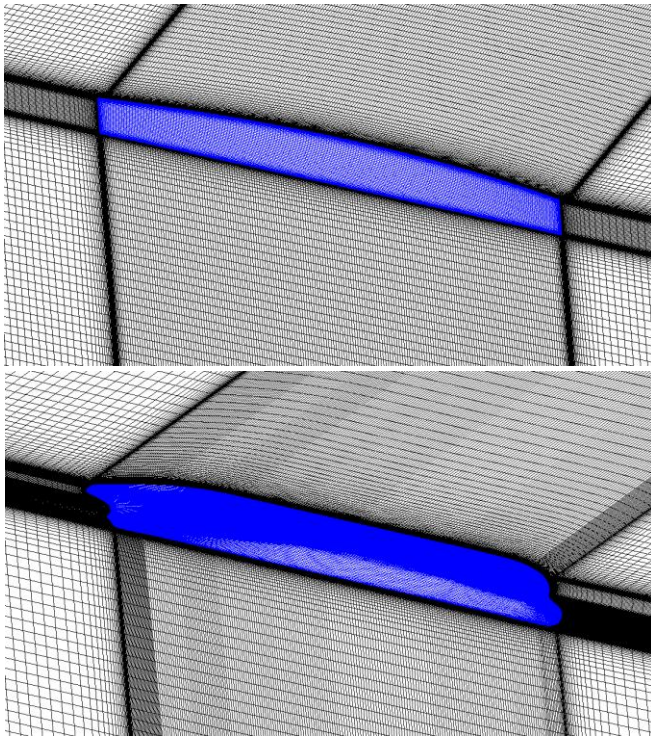Figure 2. Computation domain and boundary conditions

Figure 3. The mesh around the Wigley hull (top) and the KVLCC2 (bottom)

In simulations, the ship is fixed and water comes from the inlet boundary with ship's design velocity. Dirichlet boundary condition is set at the inlet boundary. Neumann condition is set at the outlet boundary, where the diffusion flux for all flow variables is zero. Cauchy condition is used at all symmetry planes, where the normal velocity is zero and normal gradients of all variables are zero. Non-slip wall condition is set on both ship hull and the water bottom, where the fluid has zero velocity relative to the wall. Additionally, the bottom moves with the same speed and direction with the water that comes from the inlet boundary. The treatment of the wall will be introduced in detail in the "Validation" section.

The main purpose of this study is to analyze the effects of water depth on the ship's friction. Therefore, the side boundary should be set as far as possible from the ship to avoid or keep the blockage effects at an acceptable level. To show the effects of the position of the side boundary, four calculations with the boundary L_{pp}, $2L_{pp}$, $3L_{pp}$ and $4L_{pp}$ away from the ship are performed and the results of ship's friction coefficient (C_f) are shown in Table 4. The C_f is calculated with equation (2):

$$C_f = \frac{R_f}{0.5 \cdot \rho V^2 S} \qquad (2)$$

where the R_f is the integral of the shear stress on the ship hull at x direction, ρ is water density, V is ship's design speed, and S is ship's wetted surface in still water.

Based on Table 4, it can be seen that

- When the "Side" boundary locates at L_{pp}, even though the Blockage is more than 7%, the difference of C_f is only about 1% from other cases;

- When the boundary is located at $2L_{pp}$ (Blockage < 4%), moving the boundary to a further place makes little contributions to the calculation of C_f.

Table 4 The effects of "Side" boundary's position on ship's friction ($\lg(Re) = 6.4$, $h/T = 1.2$)

Position	Blockage*	$C_f (\times 10^{-3})$	Difference
L_{pp}	7.552%	4.5511	-
$2 L_{pp}$	3.776%	4.5034	-1.048%
$3 L_{pp}$	2.517%	4.5039	-1.038%
$4 L_{pp}$	1.888%	4.5040	-1.036%

(*Blockage: the ratio between the area of ship's midsection and the area of waterway's section)

Therefore, according to this study, when the "Side" boundary is set at L_{pp} or further away from the ship hull, the blockage effects are negligible. If a higher level of accuracy is required, the blockage coefficient should be less than 4%. In this study, the Blockage < 4 % is guaranteed.

Additionally, if combined with the assumption that the velocity distribute evenly over a transverse section, i.e. a mean longitudinal velocity, another metric (γ) for blockage effects on ship's friction can be given:

$$\gamma = V_{me} / V_0 \qquad (3)$$

where the V_{me} is the mean longitudinal velocity at any transverse section, and the V_0 is the speed of water at the inlet boundary.

Corresponding to Blockage < 4 %, γ < 1.042, which indicates that if the mean longitudinal velocity is 1.042 times larger than the initial velocity, the effects of blockage on ship's friction is perceivable.

Verification

According to Eça and Hoekstra [12], the discretization error is the main error in a numerical calculation on condition that the double precision format and suitable convergence criteria are used. Those conditions can be easily guaranteed and this subsection will focus on evaluating the discretization error.

A grid refinement study, suggested by Roache [13], was performed and four geometrically similar grids were built. With a refinement factor $r = 1.25$ for all three directions, denser grids are generated and the finest grid is the G1, as shown in Table 5.

The value of $y+$ stays the same for all test cases. The results of the coefficients of frictional resistance of each grid for the Wigley hull and the KVLCC2 are shown in Figure 4.

It can be derived from Figure 4 that C_f increases slightly for the KVLCC2 but obviously for the Wigley hull with the refinement of grids (from G4 to G1). From numerical viewpoint, G1 has the highest accuracy among the four grids, but it also takes four more computing time than G2. Therefore, to balance the accuracy and the computing time, G2 is a possibly better choice. To support this assumption, the uncertainty of G2 is checked following the method of Eça and Hoekstra [14], which is shown in Table 6.
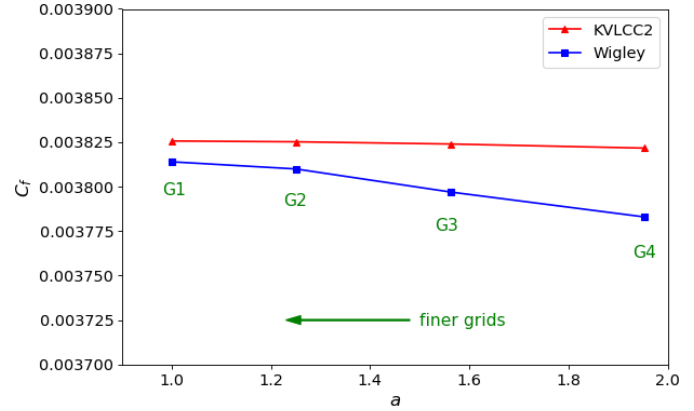

Figure 4. The results of C_f with the grid refinement for the Wigley hull and the KVLCC2 ($\lg(Re) = 6.4$, deep water)

Table 6 The uncertainty of C_f of the chosen two ships

	p	Uncertainty
Wigley hull	1.46	0.85%
KVLCC2	5.14	0.07%

(p: the order of accuracy)

The theoretical value of p is equal to the order of the method, which is equal to two in this study. The calculated p of the Wigley hull is close to this value but the corresponding p of the KVLCC2 is much higher than two. This might be caused by that the four selected grids of KVLCC2 are already at the end of the "asymptotic range", and a refinement of the mesh can no longer make and significant changes on C_f. However, the uncertainty of G2 of both the Wigley hull and the KVLCC2 has an acceptable level (less than 1%) and will be applied for further calculations.

Table 5 Number of nodes in x, y and z directions for the Wigley hull, and the KVLCC2 (deep water case, α is a factor indicating the density of mesh)

	Grids	x	y	z	α	Total cells (million)
Wigley hull	G1	558	98	122	1.00	6.45
	G2	403	78	98	1.25	3.30
	G3	350	62	78	1.56	1.69
	G4	274	50	66	1.95	0.87
KVLCC2	G1	475	102	190	1.00	9.12
	G2	379	78	158	1.25	4.78
	G3	303	62	134	1.56	2.66
	G4	243	50	118	1.95	1.58

Validation

The results of frictional resistance coefficient are compared with the ITTC57 correlation line. In the meantime, the calculations for the deep water case are performed with different values of $y+$. In the simulations, a low-Reynolds number model is used when the first grid point is in the viscous sublayer ($y+ < 5$). The wall function approach is switched on in the logarithmic layer ($30< y+ <200$). In the buffer layer ($5\leq y+ \leq 30$), a method by blending the low-Re formulation and wall functions is applied to ensure a reasonable result[15]. In the outer layer ($y+ \geq 200$), the boundary layer is still resolved with wall functions and errors will be certainly generated. However, the case when the first grid point is located in the outer layer is included for comparison.

The results of C_f in deep water against $y+$ with $\lg(Re) = 6.4$ are shown in Figure 5. Based on this figure, it can be derived that

- The values of C_f is more sensitive to $y+$ than ship types;
- When compared with the ITTC57 formula, the maximum error of the calculations is about 5%;
- The results with the $y+$ around 10 and 200 have small errors compared with the ITTC57 line.

The value of $y+$ determines the wall treatment in the simulations. Shear stress is highly depending on how the boundary layer is resolved. Therefore, C_f is sensitive to $y+$. However, in deep water, C_f of a ship hull is practically considered to be independent of ship types, and Reynolds number is the only influence factor ([1, 16]).

The ITTC57 correlation line is chosen as the benchmark since it is based on a large number of model tests and is widely accepted. For the accuracy of the calculations in this study, errors less than 5% is considered as acceptable. Therefore, the selection of $y+$ will not make a large difference and the only requirement is that the same $y+$ should be kept for different water depths with the same Reynolds number.

A $y+$ study in shallow water was practically not implemented. First, the validation is only applicable when enough validating data is available. The strategy in this study is that the code is validated in deep water and applied to gain insight into shallow water cases, where insufficient validating data is available. Secondly, once the code was verified for $y+$ in deep water case, the results can be used to predict the behavior of the code in shallow water based on a known value of $y+$.
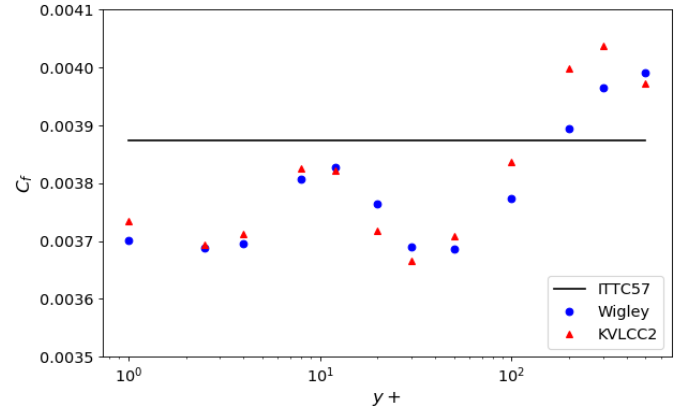

Figure 5. The results of C_f with various $y+$ and compared with the ITTC57 correlation line ($\lg(Re) = 6.4$, deep water)

RESULTS AND DISCUSSION

In this part, the results of ship's friction in extremely shallow water are shown and analyzed. Afterward, several special conditions that can affect the results are also discussed.

Results of computations and analysis

If the 2D flow is considered over a flat plate, the frictional resistance on the plate is always increasing with a decreasing gap between the two parallel plates [8]. However, this argument may not apply for 3D ship flows, especially in extremely shallow water. As shown in Figure 6, the results of the frictional resistance coefficient (C_f) of the Wigley hull and the KVLCC2 are given.

Some remarks can be made from Figure 6:

- Although the KVLCC2 and the Wigley have the similar C_f at deep water case (h/T ≈ 15), the KVLCC2 has much larger C_f when $h/T \geq 1.1$. The spreading of the curves seems to depend on the fullness of the hull lines;
- For the KVLCC2 when $\lg(Re) < 6.5$, the C_f at $h/T = 1.1$ is smaller than that at $h/T = 1.2$; for $\lg(Re) < 8.0$, the C_f at $h/T = 1.05$ is obviously less than $h/T = 1.2$. For $\lg(Re) < 6.4$, the C_f at $h/T = 1.05$ is even lower than the deep water case. This phenomenon is counterintuitive and will be explained later;
- For the Wigley hull, the C_f at $h/T = 1.1$ is always slightly larger than $h/T = 1.2$ (this may not be easily observed in the figure but it is true according to the data). For $\lg(Re) < 6.5$, slight drop of C_f can be observed for $h/T = 1.05$.
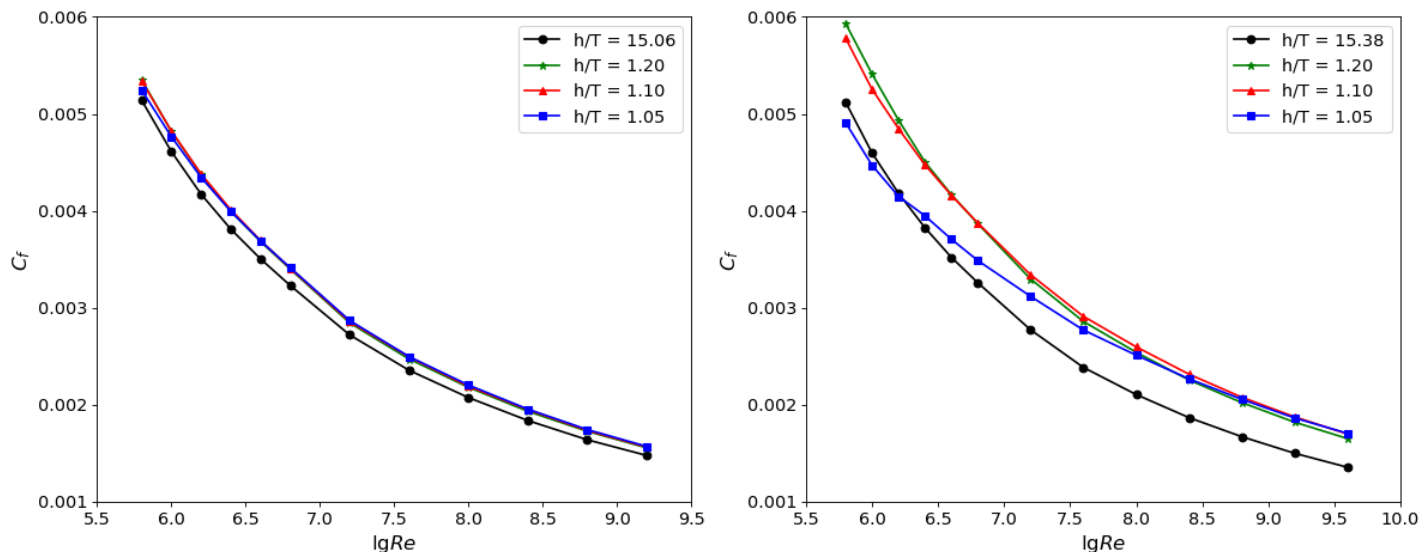
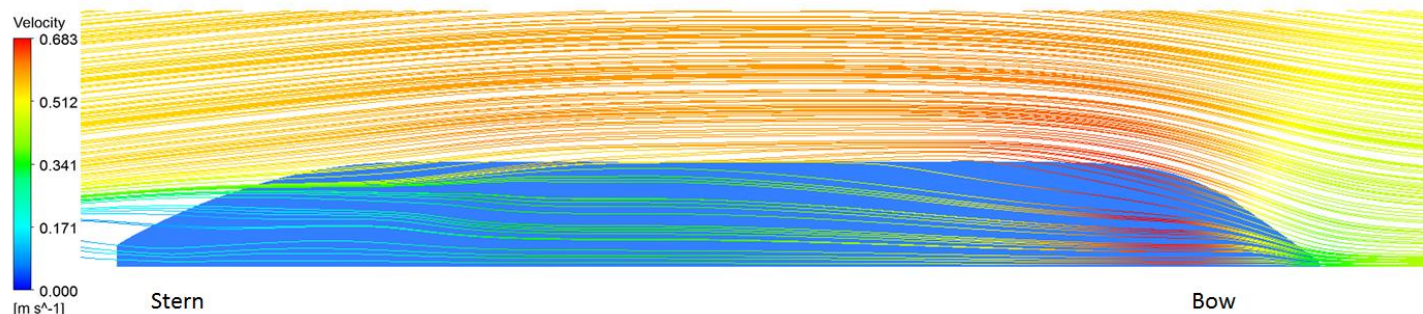Figure 6. The frictional resistance coefficient (C_f) of the Wigley hull (left) and the KVLCC2 (right)

Figure 7. Streamlines under the bottom of KVLCC2 (bottom view; streamlines at the plane -0.025T away from ship bottom plane; h/T = 1.05 and lg(Re) = 6.4)

Consequently, in contrast to the KVLCC2, the C_f of the Wigley hull is much less sensitive to the water depth. Such a difference is caused by the ship's geometry. Different from 2D cases, as the streamlines under the ship bottom shown in Figure 7, a large part of flow will go sideways if it is restricted in the vertical direction. Larger area of overspeed, therefore, can be observed beside the ship than the deep water case (Figure 8).

In the meantime, a different shape of the ship will lead to a different distribution of shear stress on the hull, as shown in Figure 9. It can be derived from Figure 9 that in contrast to the Wigley hull, a negative gradient of shear stress at –x direction is found on the flat bottom of the KVLCC2, which causes a smaller C_f in extremely shallow water. The main reason is that a

highly restricted under-keel space is formed and the boundary layer on the ship's bottom cannot be developed freely.

As depicted in Figure 10, where the velocity distribution on the midsection is shown, the development of the boundary layer on ship's bottom is highly restricted for KVLCC2 compared to the Wigley hull. Since the KVLCC2 has a much larger block coefficient (C_B = 0.81) and a large area of flat bottom, the boundary layer is highly compressed. It can be found in Figure 10 that the velocity of the flow under the bottom of the KVLCC2 decreases significantly which leads to a friction loss on the ship's bottom. Owing to a large flat bottom of the KVLCC2, such loss can lead to a smaller total frictional resistance of the ship in extremely shallow water.
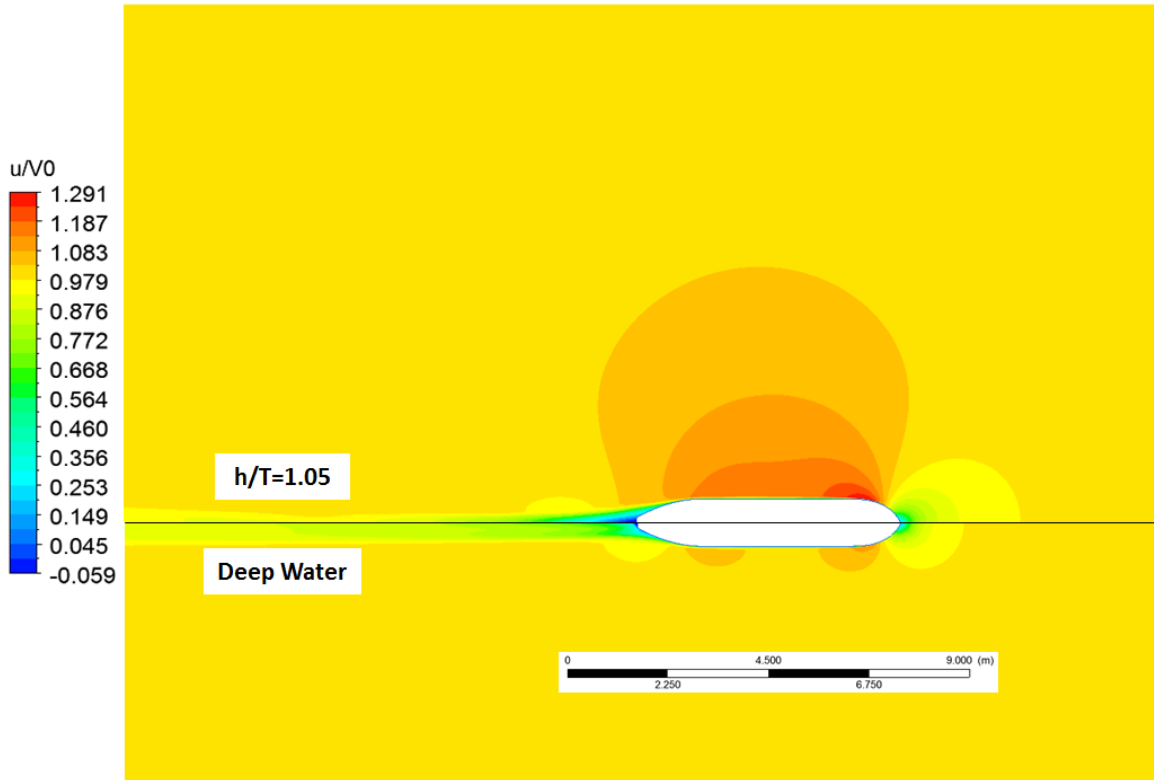
Figure 8. Velocity distribution on the plane $z = T$ around the 1/58 KVLCC2 (top: h/T=1.05; bottom: deep water; lg(Re) = 6.4; u: flow velocity at x direction; V_0: the velocity of the incoming flow)

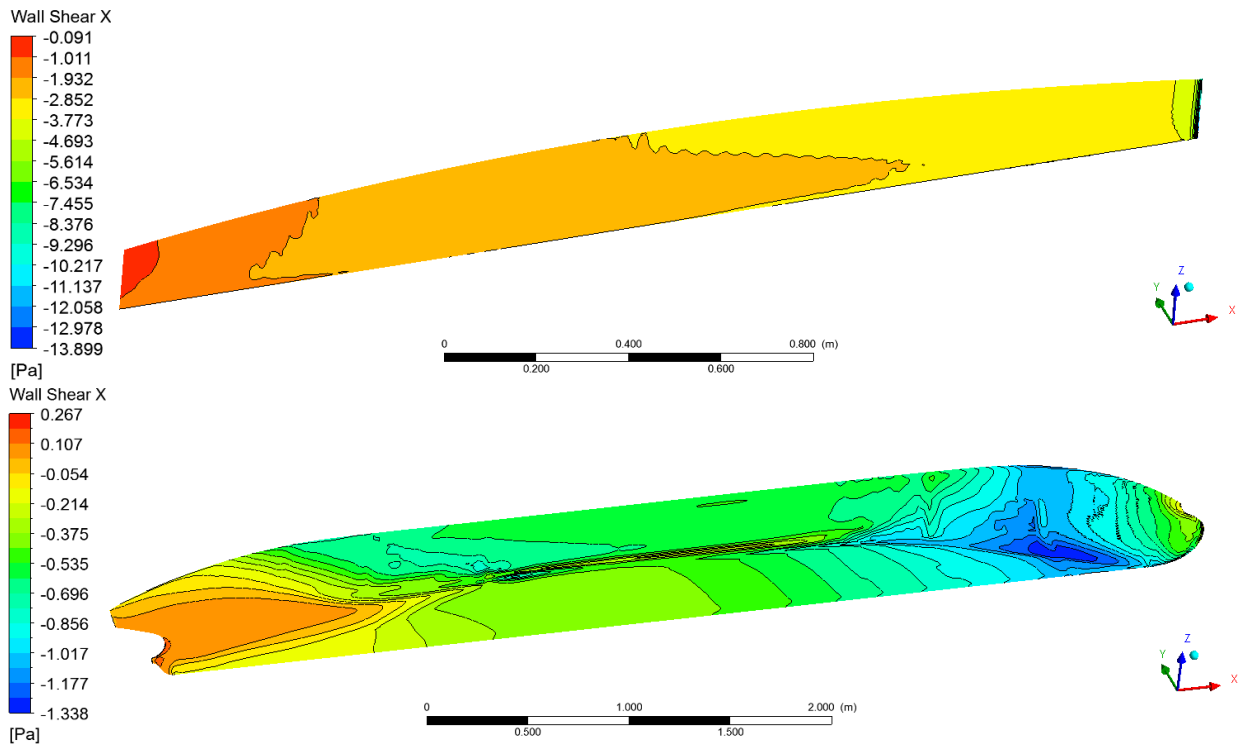Figure 9. Distribution of wall shear at x direction for the Wigley hull (top) and the 1/58 KVLCC2 (bottom) at lg(Re) = 6.4 and h/T = 1.05

7   Copyright © 2019 by ASME
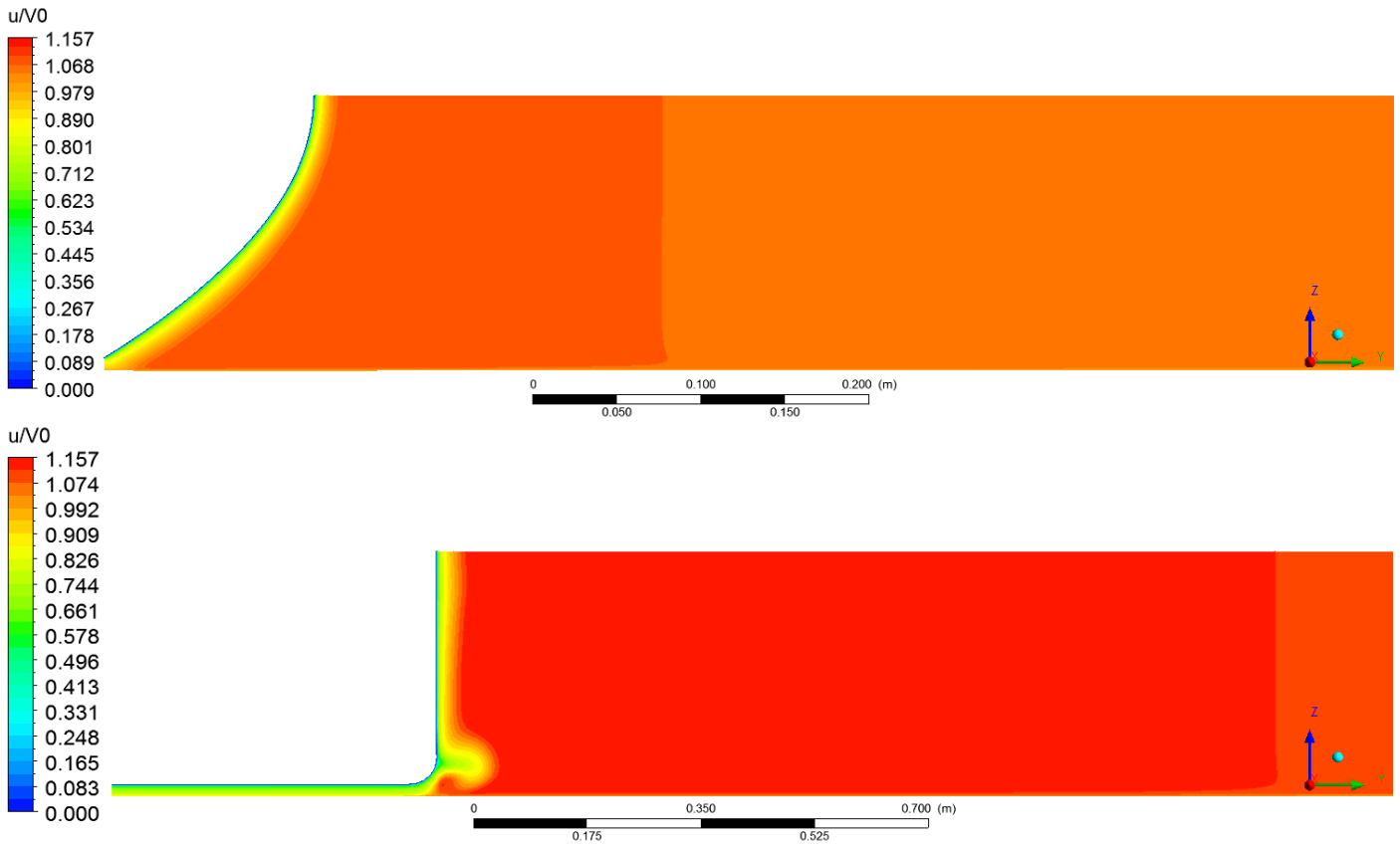
Figure 10. The velocity distribution on the midsection of the Wigley hull (top) and the KVLCC2 (bottom) at $\lg(Re) = 6.4$ and $h/T = 1.05$

An example at $\lg(Re) = 5.8$ is shown for a clear explanation. In this example, the shear force at x direction on three places: the flat bottom, the side parallel surface of the hull, and the total surface of the KVLCC2 are compared in different water depth. The surface area of each place is shown in Table 7.

Table 7 The area of the flat bottom, the side parallel surface of the hull, and the total surface of the 1/58 scaled KVLCC2

	Area(m^2)	Percentage
Bottom	1.796	43.6%
Side	1.010	24.5%
Others	1.310	31.8%
Total	4.116	100.0%

The results of shear force (friction) on each surface with different water depth are shown in Figure 11 and its percentage are visualized in Figure 12.
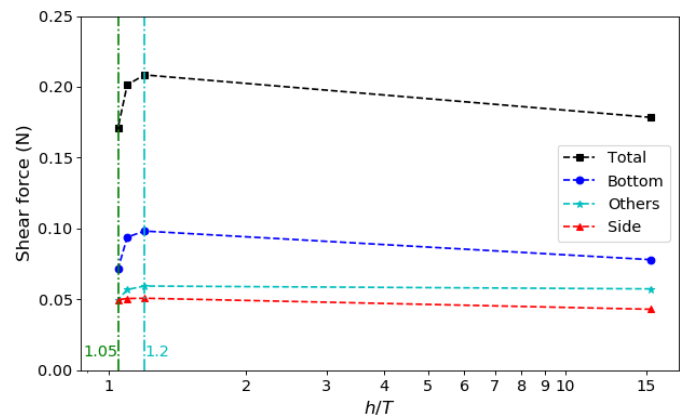

Figure 11. The shear force at x direction on the flat bottom, the side parallel surface, and the total surface of the 1/58 scaled KVLCC2 ($\lg(Re) = 5.8$)
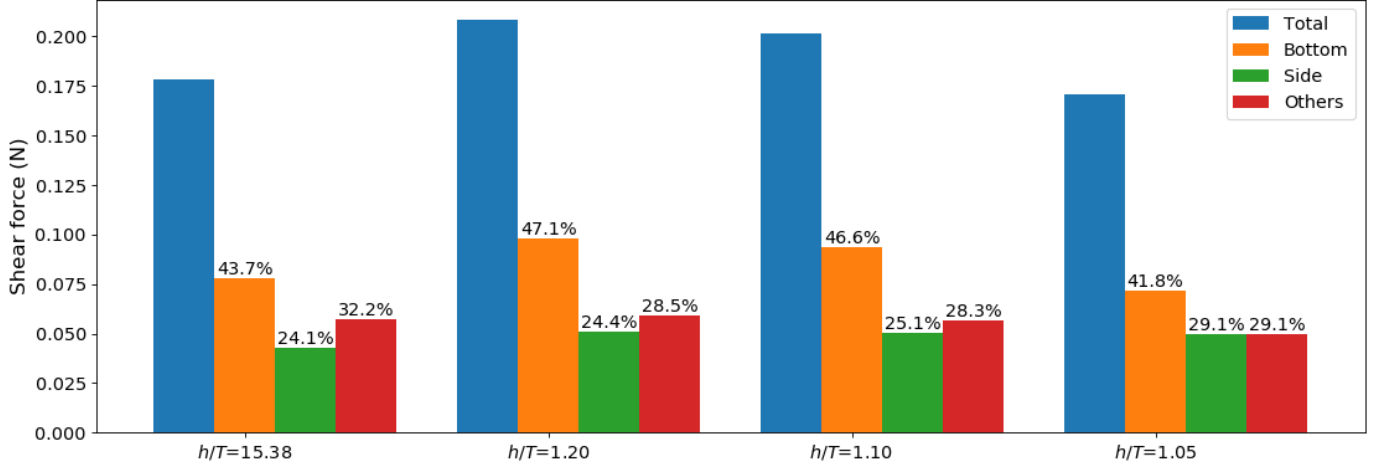
8

Copyright © 2019 by ASME

Figure 12. The shear force (N) and its percentage with different h/T on the flat bottom, the side parallel surface of the hull, and the total surface of the 1/58 scaled KVLCC2

Based on Figure 11 and 12, it can be derived that for $\lg(Re)$ = 5.8:

- Compared with the deep water (h/T = 15.38), the percentage of the friction on the flat bottom increases at h/T = 1.2, but decreased when h/T < 1.2. At h/T = 1.05, the number is even less than that in deep water;
- The shear force on the flat bottom takes about half of the total friction. For h/T < 1.2, changes of the shear force on the flat bottom dominate the changes of the total friction;
- The friction on the parallel surface and other surface is less sensitive to the water depth.

According to one's intuition, larger friction is expected if the water is shallower. However, based on this study, this is incorrect or only partly correct in extremely shallow water. This can also be explained physically by the velocity distribution as shown in Figure 10.

Flow separation is found at the stern of the KVLCC2. Vortices caused by the separation can even provide thrust locally (as shown in Figure 9). This thrust will also cause a decrease of C_f. However, the influence of the separation occurs at the stern only, which is minor compared to the changes on ship bottom (see Figure 12).

The point when the friction starts to decrease with the water depth can be predicted by comparing the ship's boundary layer in deep water with the under-keel clearance (UKC) in shallow water cases. In Figure 13, the ratio of boundary layer thickness ($\delta_{0.99}$) to ship's draft is depicted for various Reynolds numbers in deep water. The UKC of h/T = 1.10 and h/T = 1.05 are also shown in this figure. The thickness is measured at $x = 0.25L_{pp}$ (the origin is at the aft perpendicular) on the ship bottom.
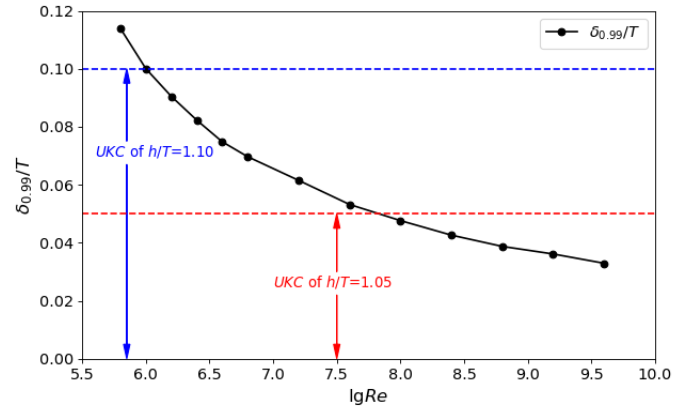

Figure 13. The ratio of bottom boundary layer thickness ($\delta_{0.99}$) to ship's draft (T) at $x = 0.25L_{pp}$ against Reynolds numbers in deep water and compared the UKC in extremely shallow water.

It can be derived from Figure 13 that

- A thinner boundary layer is observed for a higher Reynolds number;
- For h/T =1.1, the under-keel clearance (UKC) is 0.1T which is at the same order of magnitude as the boundary layer thickness at $\lg(Re)$ = 6.0. According to Figure 6, shallow water effects can spread up to $\lg(Re)$ = 6.5;
- Similarly, for h/T =1.05, the UKC is 0.05T which is similar to the $\delta_{0.99}$ at $\lg(Re)$ = 7.8, but according to Figure 6, the effects can go up to $\lg(Re)$ = 8.5.

In general, the changes of ship's frictional resistance depend on whether or not the boundary layer can be freely developed. The Wigley hull is thin enough and provides enough space for the development of the boundary layer, due to the lack of flat bottom, but it is not the case for the KVLCC2.

Discussions

- The 3D flow around a ship hull in extremely shallow water ($h/T \approx 1.1$) is so complex that it cannot be simplified into a 2D flow over a flat plate. The inherent rule of how C_f changes with water depth and Reynolds number should be studied and analyzed separately from deep and intermediate shallow waters.

- If the free surface is considered but the trim and sinkage are excluded (i.e. fixed floating position), ship-generated wave system can impact the C_f. The trough of the bow wave system, which is a primary wave system, lower the water level that close to the hull. This leads to a shallower water depth and therefore a higher C_f. The crest of the bow wave system can rise the water level but the influence is limited to a small area at the bow. The crests and troughs of the secondary wave system along the hull can compensate to each other and will make little contribution to C_f.

- If trim and sinkage are considered, they will make the under-keel clearance smaller than a designed value and let the extremely shallow case occur earlier. Additionally, trim and sinkage will also risk ships from grounding which is an unsafe condition the designer tries to avoid. Therefore, double-body computations applied in this study is conservative if compared the real navigating conditions. This conservative results have already shown significant changes of C_f in extremely shallow water, and the real cases can show even more significant changes and should be treated more carefully.

- If a ship is also restricted in the horizontal direction, i.e. sails in confined water, the side boundary will play a similar role as the water bottom. When the limitations from the two directions are at the same order of magnitude, the flow passes over both the bottom and the side surface are comparable to a 2D flow over a flat plate, and the conclusions derived from 2D cases may apply again.

CONCLUSIONS

In this study, the frictional resistance of a Wigley hull and the KVLCC2 in extremely shallow water are obtained with double-body computations. The effects of extremely shallow water on the ship's friction are demonstrated and compared with the results in deep and intermediate shallow water. Several conclusions can be derived based on the analysis:

- Against to one's intuition, when $h/T < 1.2$ and at a relatively low Reynolds number, the friction of a highly-curved ship (such as the KVLCC2) is decreasing with decreasing water depth. These changes usually occur on the model scale of ships;

- For slender ships like the Wigley hull, in contrast to the KVLCC2, only slight effects can be observed when the water is as shallow as $h/T < 1.2$;

- The geometry of a ship plays an important role in the prediction of the frictional resistance in extremely shallow water. Evaluating whether the boundary layer can develop freely is the key to estimate the trend of changes;

- Due to a different rule from deep and intermediate shallow water, the prediction of ship's friction in extremely shallow water should be considered specifically and separately. Both the geometry and the Reynolds number should be considered if a new prediction method is built.

With the calculations of ship's friction in extremely shallow water, this study adds some information into the understanding of the physics and the prediction of ship's friction in extremely shallow water which expects to improve the prediction of ship's resistance in shallow water.

REFERENCES

[1] ITTC, 1957, Proc. 8th International Towing Tank Conference.

[2] Zeng, Q., Hekkenberg, R., Thill, C., and Rotteveel, E., 2017, "Numerical and experimental study of resistance, trim and sinkage of an inland ship model in extremely shallow water.," International Conference on Computer Applications in Shipbuilding (ICCAS2017), RINA, Singapore, pp. 19-25.

[3] Schlichting, O., 1934, "Ship resistance in water of limited depth-resistance of sea-going vessels in shallow water (translated by Roemer, M.C, 1940)," Jahrbuch der STG, 35, pp. 127-148.

[4] Lackenby, H., 1963, "The effect of shallow water on ship speed," Shipbuilder and Marine Engineer, 70, pp. 446-450.

[5] Jiang, T., 2001, "A new method for resistance and propulsion prediction of ship performance in shallow water," Proc. Proceedings of the 8th International Symposium on Practical Design of Ships and Other Floating Structures.

[6] Raven, H., 2012, "A computational study of shallow-water effects on ship viscous resistance," Proc. 29th symposium on naval hydrodynamics, Gothenburg.

[7] Eloot, K., and Vantorre, M., 2011, "Ship behaviour in shallow and confined water: an overview of hydrodynamic effects through efd," Specialists' Meeting on Assessment of Stability and Control Prediction Methods for Air and Sea Vehicles (AVT-189/RSM-028)Portsdown, United Kingdom.

[8] Zeng, Q., Thill, C., Hekkenberg, R., and Rotteveel, E., 2018, "A modification of the ITTC57 correlation line for shallow water," Journal of Marine Science and Technology, pp. 1-16.

[9] Kajitani, H., Miyata, H., Ikehata, M., Tanaka, H., Adachi, H., Namimatsu, M., and Ogiwara, S., 1983, "The summary of the cooperative experiment on Wigley parabolic model in Japan," TOKYO UNIV (JAPAN).

[10] Kim, W., Van, S., and Kim, D., 2001, "Measurement of flows around modern commercial ship models," Experiments in fluids, 31(5), pp. 567-578.

[11] Menter, F. R., 1994, "Two-equation eddy-viscosity turbulence models for engineering applications," AIAA journal, 32(8), pp. 1598-1605.

[12] Eça, L., and Hoekstra, M., 2009, "Evaluation of numerical error estimation based on grid refinement studies with the method of the manufactured solutions," Computers & Fluids, 38(8), pp. 1580-1591.

[13] Roache, P. J., 1998, Verification and validation in computational science and engineering, Hermosa, Albuquerque, New Mexico.

[14] Eça, L., and Hoekstra, M., 2014, "A procedure for the estimation of the numerical uncertainty of CFD calculations based on grid refinement studies," Journal of Computational Physics, 262, pp. 104-130.

[15] ANSYS, 2017, "ANSYS® Academic Research, Release 18.1, Help System, Fluent Theory Guide," Ansys Inc.

[16] ITTC, 2011, "The Resistance Committee: Final Report and Recommendations," Proc. 26th International Towing Tank Conference, pp. 1-50.